Fig. S1

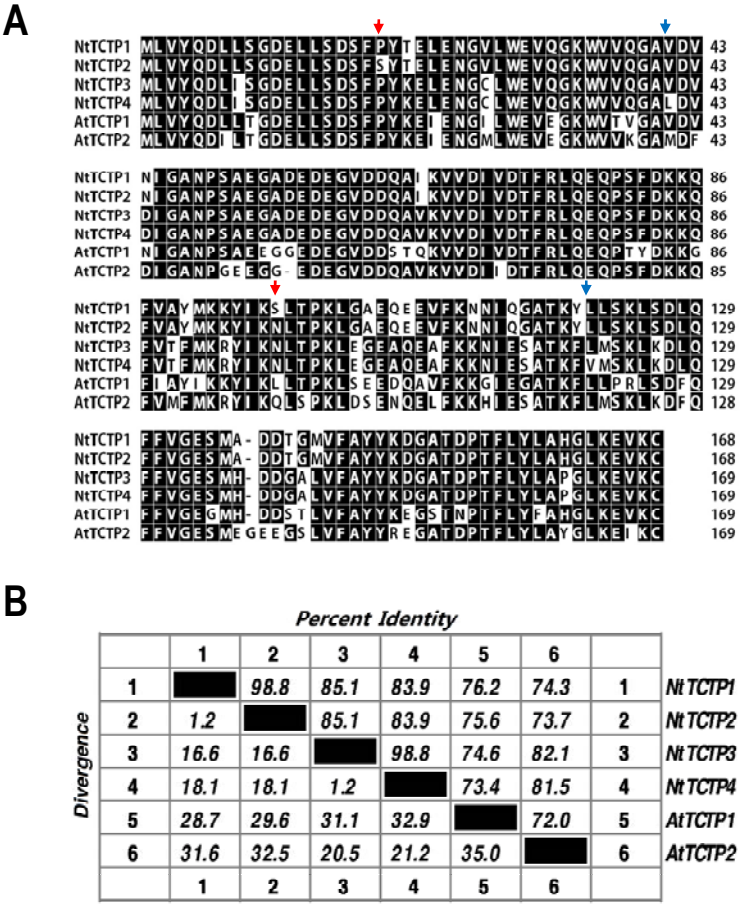

Figure S1. Sequence comparison among TCTPs from tobacco and Arabidopsis.

(A) Sequence alignment using clustal w method (Lasergene.v7.1). Conserved amino acids were shaded in black. Red arrows indicate the variations between two homologs of NtTCTP (NtTCTP1 and NtTCTP2); blue arrows indicate the variations between two homologs of NtTCTPL (NtTCTP-like: NtTCTP3 and NtTCTP4).

(B) Sequence identity analysis among TCTPs from tobacco and Arabidopsis. It shows that NtTCTP1 and NtTCTP2 are more similar to AtTCTP1, while NtTCTP3 and NtTCTP4 are more similar to AtTCTP2.

Accession: NtTCTP1 (gene_19203, KM507327), NtTCTP2 (gene_40052), NtTCTP3 (gene_60507) and NtTCTP4 (gene_60645) are from the Ntab-BX_AWOK-SS_Basma.proteins.faa database on sol genomics network; AtTCTP1 (NP_188286), AtTCTP2 (NP_187205).

Fig. S2

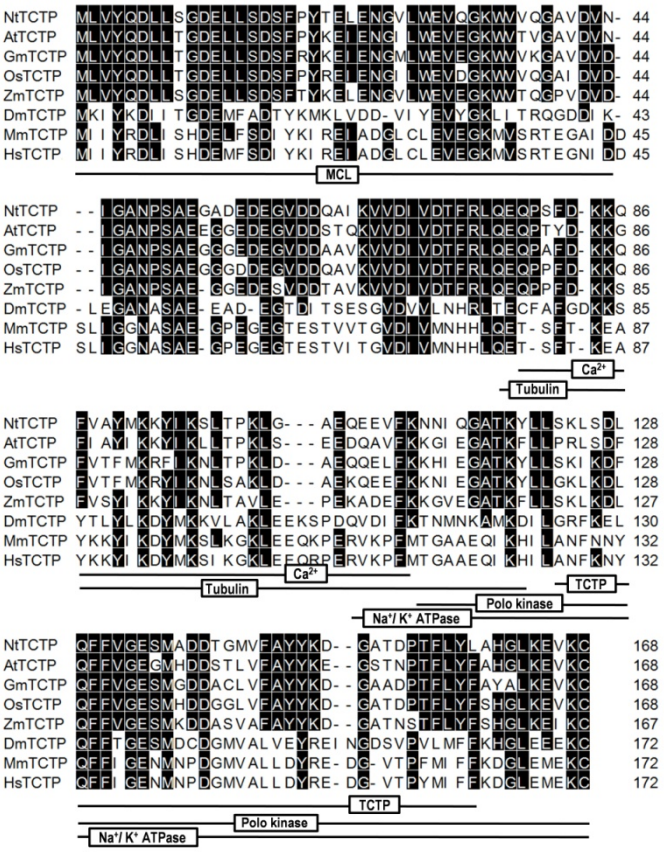

Figure S2. Sequence comparison of NtTCTP with other TCTPs from plants and animals. Sequence alignment was performed using clustal w method from Lasergene.v7.1. Conserved amino acids were shaded in black. The MCL, tubulin binding, Ca^{2+} binding, Na^{+}/K^{+} ATPase interaction, polo kinase interaction and TCTP self-interaction domains identified in nonplant TCTPs were indicated by black underlines. Accession numbers: NtTCTP (KM507327), AtTCTP (NP_188286), GmTCTP (NP_001237819), OsTCTP (NP_001068405), ZmTCTP (NP_001105104), DmTCTP (NP_650048), MmTCTP (NP_033455), HsTCTP (NP_003286).

Fig. S3

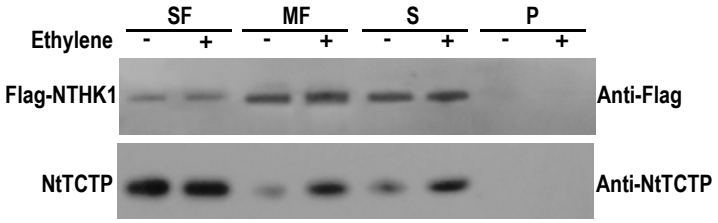

Figure S3. Examination the solubility of Flag-NTHK1 and NtTCTP proteins in membrane resuspension buffer used for co-IP assay. Membrane fraction was separated from soluble fraction as described in the methods under *co-immunoprecipitation (co-IP)*. After dissolving in membrane resuspension buffer for 1 h on ice, 200 μg membrane fraction was centrifuged at 150,000 for 1 h, then 5% of the supernatant (S) and 10% of the resuspended pellet (P), with the addition of 10 μg membrane fraction (MF) and 10 μg soluble fraction (SF), were separated by SDS-PAGE and followed by immunoblotting assay using anti-Flag and anti-NtTCTP antibodies to detect Flag-NTHK1 and NtTCTP respectively. The absence of signal in the pellet indicates that Flag-NTHK1 and NtTCTP proteins were solubilized fully in the membrane resuspension buffer. For ethylene treatment, tobacco seedlings were placed in sealed boxes fulfilled with 100 $\mu L.L^{-1}$ (+) or 0 $\mu L.L^{-1}$ (-) ethylene for 3 h.

Fig. S4

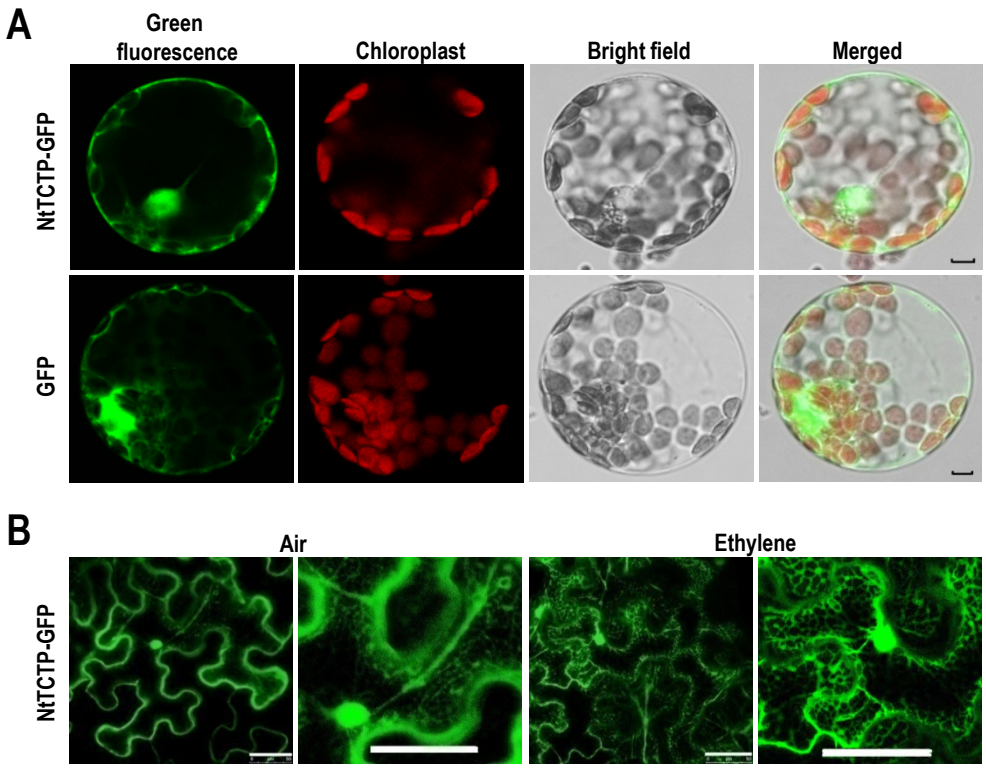

Figure S4. Subcellular localization of NtTCTP was revealed by GFP fusion in different expression systems.
(A) Subcellular localization of NtTCTP in tobacco protoplasts. Bar = 5 μm.
(B) Subcellular localization of NtTCTP in *N. benthamiana* leaf epidermal cells. Bar = 50 μm.
The GFP signal was detected with confocal microscopy system. In both expression systems, the GFP signal could be observed in nucleus and cytoplasm, but subtle exploration in tobacco leaf epidermal cells indicated the partial localization of NtTCTP at ER, and it was enhanced by ethylene treatment (100 $\mu L.L^{-1}$ for 3 h).

Fig. S5

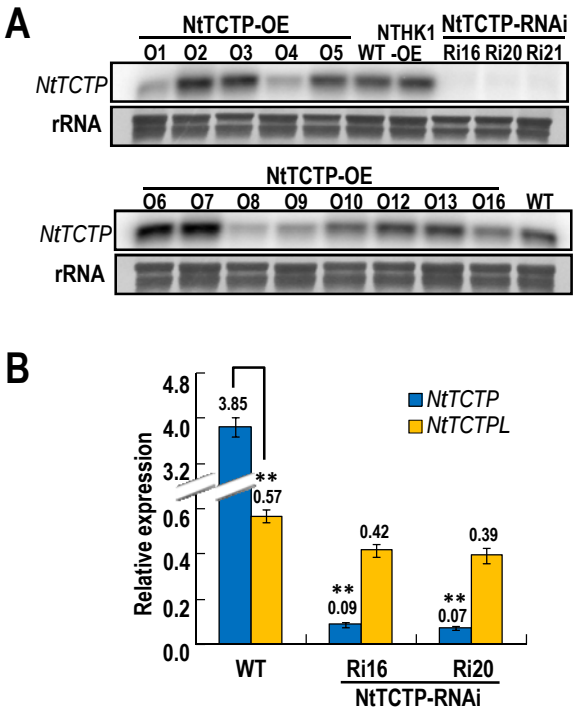

Figure S5. Expression analysis of *NtTCTPs* in transgenic tobacco lines.

(A) Northern blotting analysis of *NtTCTP* expression level in different tobacco lines. All transgenic tobacco lines were first selected by RT-PCR on mRNA level, then a series of overexpression lines and three RNA interference lines were re-identified by northern blotting (20 μg of total RNA per lane). Finally, two *NtTCTP*-overexpressing (O2 and O7) and two *NtTCTP*-silencing (Ri16 and Ri20) lines were used for genetic and functional analysis.

(B) Expression analysis of all tobacco *TCTPs* in selected *NtTCTP*-silencing lines by qRT-PCR. Expression levels of *NtTCTPs* were normalized to *NttubA1*. The data are expressed as the mean ± SD from three samples. Student's *t*-tests between the WT and *NtTCTP*-silencing plants were performed (**, $P < 0.01$). Differential expression analysis between *NtTCTP* (*NtTCTP1* and *NtTCTP2*) and *NtTCTPL* (*NtTCTP-like*: *NtTCTP3* and *NtTCTP4*) in the WT plants was conducted using student's *t*-test (**, $P < 0.01$). Three biological replicates were performed with similar results, and one of them was shown.

WT, wild type tobacco; NTHK1-OE, the *NTHK1*-overexpressing line; NtTCTP-OE, *NtTCTP*-overexpressing line; NtTCTP-RNAi, *NtTCTP*-silencing line.

Fig. S6

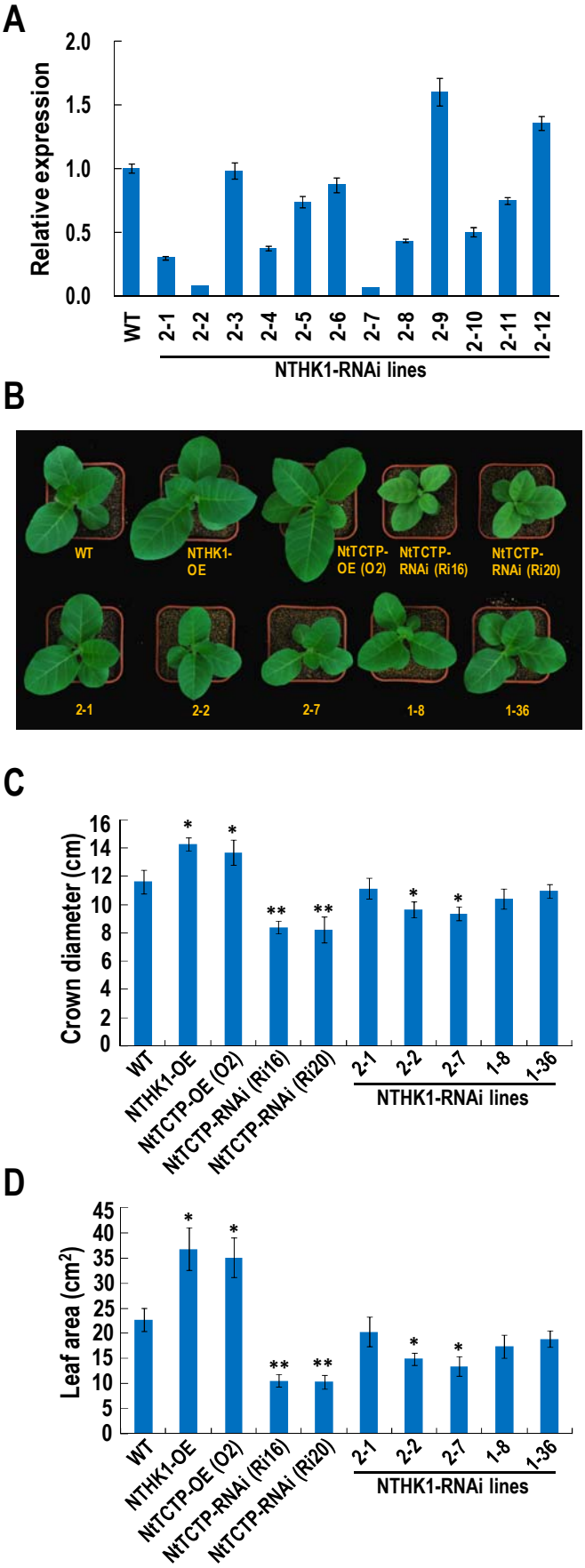
A
Relative expression
2.0
1.5
1.0
0.5
0.0
WT
2-1
2-2
2-3
2-4
2-5
2-6
2-7
2-8
2-9
2-10
2-11
2-12
NTHK1-RNAi lines
B
WT
NTHK1-OE
NtTCTP-OE (O2)
NtTCTP-RNAi (Ri16)
NtTCTP-RNAi (Ri20)
2-1
2-2
2-7
1-8
1-36
C
Crown diameter (cm)
16
14
12
10
8
6
4
2
0
WT
NTHK1-OE
NtTCTP-OE (O2)
NtTCTP-RNAi (Ri16)
NtTCTP-RNAi (Ri20)
2-1
2-2
2-7
1-8
1-36
NTHK1-RNAi lines
D
Leaf area (cm2)
45
40
35
30
25
20
15
10
5
0
WT
NTHK1-OE
NtTCTP-OE (O2)
NtTCTP-RNAi (Ri16)
NtTCTP-RNAi (Ri20)
2-1
2-2
2-7
1-8
1-36
NTHK1-RNAi lines

Figure S6. RNA interference analysis of *NTHK1* in tobacco.

(A) qRT-PCR analysis of the *NTHK1* expression level in *NTHK1*-silencing transgenic lines. Two transcript regions of *NTHK1* (type 1: from 2125 bp to 2630 bp; type 2: from 1382 bp to 1904 bp) were used to form two different pZH01 constructs for *NTHK1*-silencing transgene. Type 1 *NTHK1*-silencing transgenic lines were analyzed previously in our lab (Cao et al., 2015). Expression levels of *NTHK1* were normalized to *NttubA1* and were relative to the WT. The data are expressed as the mean ± SD from three samples. *NTHK1*-silencing lines of 2-1, 2-2 and 2-7, with the addition of 1-8 and 1-36 (Cao et al., 2014) were selected for further experiments.

(B) Comparison of the growth of different tobacco lines. Photograph shows the 36-DAS-old seedlings of different tobacco lines (*NTHK1*-silencing lines are showed at down column). The pot size is 8 cm × 8 cm.

(C) Measurement of seedling size at different stages.

(D) Measurement of the sixth true leaf area from 36-DAS-old tobacco plants.

For (C) and (D), each data point is means ± SE from three biological replicates (each replicate has 10 seedlings). Asterisk indicates a significant difference from the WT (*t*-test; *, $P < 0.05$; **, $P < 0.01$). NTHK1-OE, the *NTHK1*-overexpressing line; NtTCTP-OE, *NtTCTP*-overexpressing line O2; NtTCTP-RNAi, *NtTCTP*-silencing line Ri20; NTHK1-RNAi, *NTHK1*-silencing lines.

Fig. S7

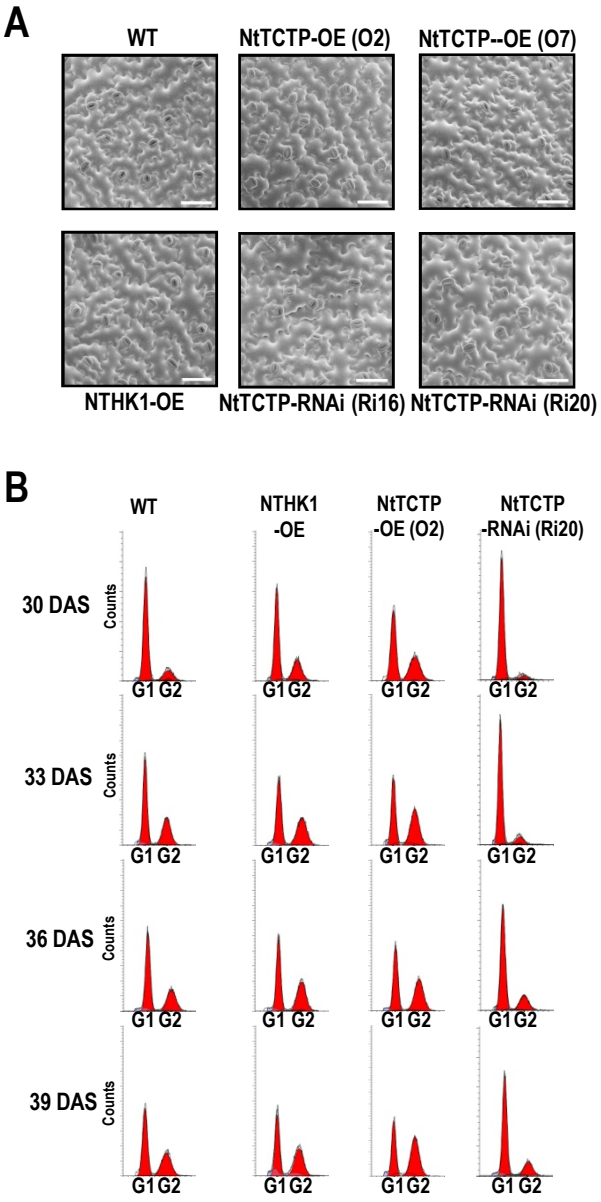

Figure S7. SEM and flow cytometric analysis of leaf cells from different tobacco lines.

(A) Scanning electron micrograph of leaf upper epidermal cells. The sixth true leaves from 48-DAS-old (DAS, days after stratification) tobacco plants were collected for SEM analysis. Bar = 100 μm.

(B) Flow cytometric analysis of DNA contents in the sixth true leaf cells at different stages.

NTHK1-OE, the *NTHK1*-overexpressing line; NtTCTP-OE, *NtTCTP*-overexpressing line; NtTCTP-RNAi, *NtTCTP*-silencing line.

Fig. S8

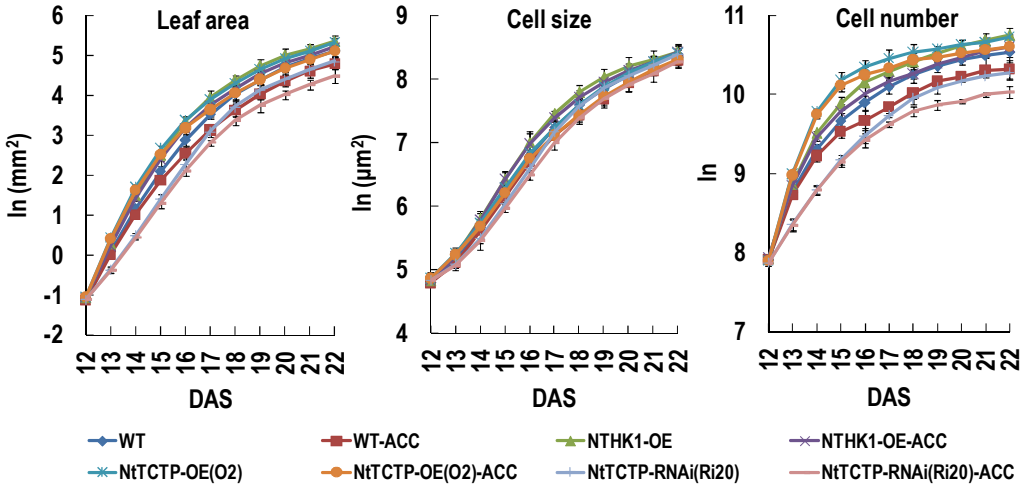

Figure S8. Leaf area, cell size and cell number of different tobacco lines in the presence or absence of ethylene precursor ACC. At the stage of 12 DAS, the third true leaves of all tobacco lines begin to sprout out. Then seedlings were transplanted to control or ACC-containing medium for further growth, and the third true leaves were collected every day for measurements of leaf area, cell size and cell number. The data are expressed as the mean ± SE from three independent experimental groups. For leaf area, 8 leaves per group were measured. For cell size and cell number calculation, the upper epidermis of 4 leaves from each group were photomicrographed and analyzed using ImageJ 1.38X, and four independent areas averaged between the apical and basal positions were examined and at least 30 cells per area were measured.

WT, wild type tobacco; NTHK1-OE, the *NTHK1*-overexpressing line; NtTCTP-OE, *NtTCTP*-overexpressing line; NtTCTP-RNAi, *NtTCTP*-silencing line.

Fig. S9

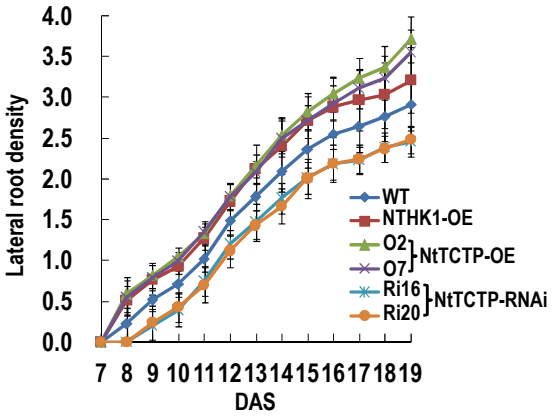

Figure S9. Lateral root density in different tobacco lines. Lateral root density was calculated by dividing the lateral root number by the primary root length (the same data as in figure 7). The result showed *NtTCTP*-silencing lines were significantly decreased while *NtTCTP*-overexpressing lines were significantly increased compared to wild type in the whole observation period (*t*-test, $P < 0.05$). However, root density of the *NTHK1*-overexpressing line was only increased significantly before 12 DAS (*t*-test, $P < 0.05$).

WT, wild type tobacco; NTHK1-OE, the *NTHK1*-overexpressing line; NtTCTP-OE, *NtTCTP*-overexpressing line; NtTCTP-RNAi, *NtTCTP*-silencing line.

Fig. S10

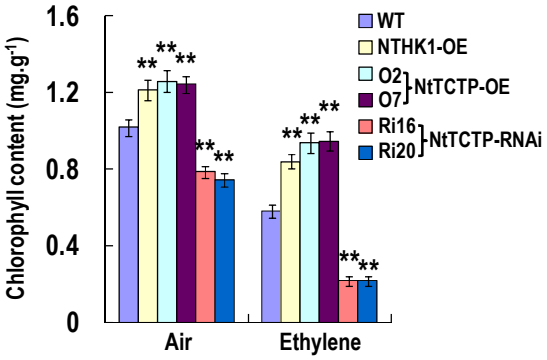

Figure S10. Chlorophyll contents in leaves of various plants treated with ethylene or air. The sixth true leaves from 60-DAS-old plants were treated with 100 μL.L^{-1} ethylene in sealed boxes for 5 days to induce senescence. After treatment, chlorophyll contents were measured to reflect the extent of leaf senescence. The data are expressed as the mean ± SE from three independent experimental groups (6 leaves per group), and double asterisks indicate a significant difference from the WT (*t*-test, $P < 0.01$).

WT, wild type tobacco; NTHK1-OE, the *NTHK1*-overexpressing line; NtTCTP-OE, *NtTCTP*-overexpressing line; NtTCTP-RNAi, *NtTCTP*-silencing line.

Fig. S11

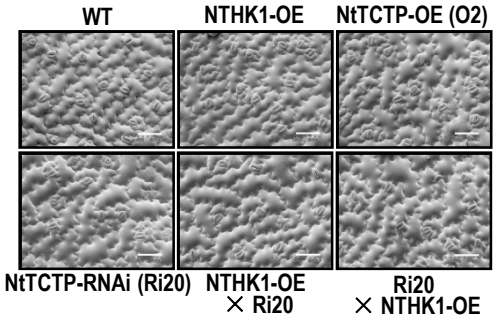

Figure S11. Scanning electron micrograph of leaf upper epidermal cells from different tobacco lines. The sixth true leaves from 48-DAS-old tobacco plants were collected for SEM analysis of leaf upper epidermal cells (bar = 100 μm).

WT, wild type tobacco; NTHK1-OE, the *NTHK1*-overexpressing line; NtTCTP-OE, *NtTCTP*-overexpressing line; NtTCTP-RNAi, *NtTCTP*-silencing line.